Surface characterisation of silicon substrates seeded with diamond nanoparticles under UHV annealing

Non Peer-reviewed author version

Arnault, J.C.; Saada, S.; WILLIAMS, Oliver; HAENEN, Ken; Bergonzo, P.; NESLADEK, Milos; Polini, R. & Osawa, E. (2008) Surface characterisation of silicon substrates seeded with diamond nanoparticles under UHV annealing. In: PHYSICA STATUS SOLIDI A-APPLICATIONS AND MATERIALS SCIENCE, 205(9). p. 2108-2113.

DOI: 10.1002/pssa.200879728
Handle: http://hdl.handle.net/1942/8549

Surface characterisation of silicon substrates seeded with diamond nanoparticles under UHV annealing

J.C Arnault[*,1], S. Saada[1], O. A. Williams[2, 3], K. Haenen[2, 3], P. Bergonzo[1], M. Nesladek[1], R. Polini[4] and E. Osawa[5]

[1] CEA, LIST, Diamond Sensor Laboratory, Gif sur Yvette, F-91191 France;
[2] Institute for Materials Research (IMO), Hasselt University, Belgium
[3] Division IMOMEC, IMEC vzw, Belgium
[4] Dipartimento di Scienze e Tecnologie Chimiche, Università di Roma Tor Vergata,Italy
[5] NanoCarbon Research Institute, Ltd., Asama Research Extension Centre, Shinshu University, Japan

Received zzz, revised zzz, accepted zzz
Published online zzz (Dates will be provided by the publisher.)

PACS 00.00.Xx, 11.11.Yy, 22.22.Zz, 33.33.Aa (Please insert 4 to 6 PACS codes from the enclosed list or from www.aip.org/pacs)

* Corresponding author: jean-charles.arnault@cea.fr, Phone: +00 33 1 69 08 71 02, Fax: +00 33 1 69 08 91 75

The thermal stability of Ultra Dispersed Diamond on silicon surfaces has been investigated. Samples have been annealed under Ultra-High Vacuum conditions. The evolution of the carbon binding states at the surface has been monitored sequentially by XPS and XEELS. After annealing at 1173 K, sp^3 seeds present initially have been significantly modified. Contrary to lower temperature, no diamond has been detected either by XPS or by FEG-SEM after a short growth step. XPS spectra indicate the formation of silicon carbide.

This is the caption of the **optional** abstract figure. If there is no figure here, the abstract text will fill both columns.

1 Introduction

Ultra Dispersed Diamond (UDD) powders have focused a great interest during the last years. Indeed, the diamond nanoparticles are good candidates for the transport of biological molecules to cells [1]. For this application, the main challenge is the control of their functionalisation. Moreover, these nanometer-sized particles have been used to perform seeding of surfaces to initiate diamond growth [2]. Via this procedure, a high density of diamond seeds (10^{10}-10^{11} / cm^2) can be provided on the substrate prior to CVD growth. Important efforts are at the present time concentrated on the UDD dispersion in liquid suspension [3, 4]. The main objective is to prevent the aggregation occurring in the liquid media. Another point less studied previously is related to the stability of diamonds seeds on the substrate. Especially, their behaviour under plasma conditions during the early stages of growth. Our first study dealing with the surface modifications of silicon nanoseeded surfaces under H_2 plasma has recently underlined the excellent stability for UDD after H_2 Microwave Plasma Chemical Vapour Deposition (MPCVD) performed at 1213 K. During the CVD exposure, chemical interactions with reactive species (etching, carbon redeposition, surface passivation,…) and thermal activated mechanisms (carbon diffusion into silicon, transformation of diamond nanoparticles) are taking place simultaneously at the surface. To better understand the unexpected stability under H_2 plasma, it is required to separate both mechanisms. The main aim of the present paper is to investigate the thermal stability of UDD on Si surfaces. Thermal treatments have been carried out under Ultra-High Vacuum (UHV) condi-

tions up to 1173 K. A short MPCVD exposure using a CH_4 / H_2 mixture was then applied to Si surfaces seeded with UDD to allow the growth of the remaining sp^3-carbon growth sites. The evolution of the surface species was monitored by in situ surface analysis carried out sequentially (nanoseeding / annealing / CVD growth). X-ray Photoelectron (XPS) and X-ray Electron Energy Loss (XEELS) Spectroscopies were used. Field Emission Gun Scanning Electron Microscopy (FEG-SEM) investigations were then performed to correlate the density of remaining sp^3-carbon growth sites to XPS analysis. After the thermal treatment performed at 1173 K, no diamond was detected either by XPS or by FEG-SEM, suggesting the most part of diamond nanoparticles have been transformed.

2 Experimental

Nanoseeding was performed on silicon (100) samples according to the procedure previously described [3].

Experiments were carried out in an UHV system connected to a microwave CVD reactor. Three different samples were considered. The first nanoseeded Si sample underwent directly a CVD growth step to get a reference for the density of sp^3-carbon growth sites. Thermal treatments achieved at 1073 K and 1173 K were applied during 60 min to the two other samples. During the annealing, the pressure in the chamber was lower than 5. 10^{-9} hPa.

Surface analysis was performed using XPS with an Al Kα monochromatized anode (hν = 1486.6 eV). The binding energy scale was calibrated versus the Au 4f 7/2 peak located at 84.0 eV. The evolution of the carbon and silicon binding states was followed recording Si 2p and C 1s core levels. The XPS ratios P_x/C_{total} (%) corresponding to the integrated intensity of each peak P_x over the total area of the C 1s spectrum was calculated. XPS Si 2p to C 1s ratio and Si 2p to O 1s ratio were considered: the first one is a fingerprint of the carbon amount at the surface while the second is related to the silicon oxide stability. In addition to Si 2p and C 1s core levels, XEELS spectra were recorded at the carbon core level to give additional informations about the carbon binding state. A short growth step was performed by MPCVD (CH_4 (0.6 %) / H_2) to reveal the sp^3 seeds preserved after the UHV annealing. During the growth step, the total pressure was 30 hPa, the microwave power was 550 W. The surface temperature measured by an optical pyrometer was 993 K. High Resolution SEM investigations were performed using a LEO Supra 35 equipped with a Field Emission Gun providing a high brilliance and a lateral resolution lower than 10 nm for our samples. The images were recorded using an acceleration voltage of 15 kV.

3 Results

3.1 Initial Si(100) nanoseeded surface

The initial seeded surface has been investigated using XPS. The carbon core level spectrum is shown on figure 1a. The broad C1s peak suggests the presence of several carbon binding states. The four main components observed at 285 eV, 285.8 eV, 286.5 eV and 287.3 eV are assigned to C-C sp^2, C-C sp^3, C-OH and C-O-C bonds, respectively [5]. Their P_x/C_{total} ratios were 28 %, 27 %, 20 % and 15 %, respectively. The two weaker components detected at higher binding energy are corresponding to C=O (288.2 eV) and OH-C=O (289.2 eV) bonds. The carbon binding state associated with the peak located at 284.5 eV could be assigned to oxycarbides. The part of carbon adsorbed on uncovered Si is negligible. It has been checked by XPS on a Si sample which underwent the ultrasonic treatment without UDD.

This XPS carbon core level is well correlated with Transmission Electron Microscopy investigations which revealed that UDD exhibit a sp^3-carbon core surrounded by a sp^2-carbon defective shell [6]. Moreover, previous Fourier Transform Infrared (FTIR) spectra underlined that UDD termination involves the presence of hydroxyls (C-OH), ether (C-O-C) and carbonyls (C=O) groups [7-8] resulting from the severe acid treatment applied prior the dispersion of diamond nanoparticles in water.

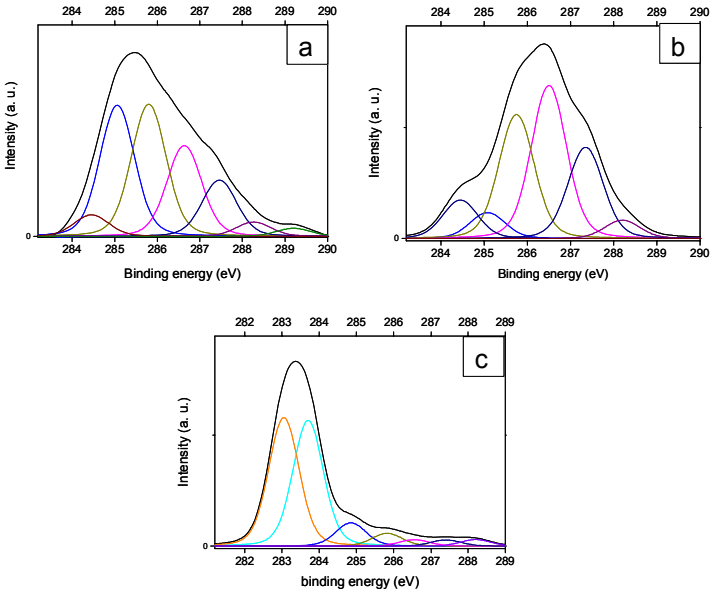

Figure 1 XPS C1s core level spectra a) initial state; after an UHV treatment b) at 1073 K; c) at 1173 K.

The morphology of the nanoseeded surface is depicted on the figure 2. The SEM-FEG picture well emphasized the aggregation of UDD dispersed on the silicon surface. The surface covered by diamond nanoparticles is close to 17 %. The density of sp^3-carbon seeds extracted by image analysis is 2.10^{11} / cm^2. As the major part of the silicon surface remained uncovered, Si peaks are detected in the XPS spectra. At the Si 2p core level, components corresponding to oxidized silicon were observed.

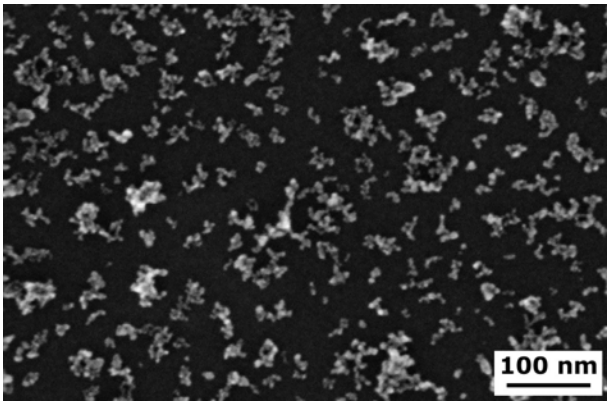

Figure 2 FEG-SEM picture of the initial seeded Si surface

3.2 UHV annealing at 1073 K

This thermal treatment led to a significant decrease of the carbon amount at the surface. Indeed, the C 1s / Si 2p ratio is reduced by a 1/3 factor. This suggests a thermally induced desorption process.This trend has been observed for annealing performed at lower temperature close to 800 K (not shown). At the carbon core level (figure 1b), the sp^2-carbon component was the most affected. Its P_x/C_{total} ratio drops from 28 % to 6 %. The desorbed carbon is thus mostly sp^2 hybridised. On the other hand, the contribution of the sp^3-carbon peak is most weakly affected. Nevertheless, this annealing temperature is insufficient to remove carbon / oxygen bonds. Hydroxyls and ether groups were major contributions. According to the Si 2p core level (figure 3a), the silicon oxide is still present at the surface. The corresponding component was located at + 4 eV from the Si contribution (99.6 eV). This is in agreement with the stable Si 2 p / O 1s ratio. Its thickness has been estimated to 2.3 nm from the ratio of the respective XPS intensities (figure 3a).

3.3 UHV annealing at 1173 K

The surface underwent major modifications. The carbon core level spectrum has been deeply modified (figure 1c): the two main components are now corresponding to silicon carbide and carbon-terminated SiC located at 283.1 eV [9] and 283.7 eV [10], respectively. Both represent 87 % of the carbon amount at the surface. This is confirmed by the XEELS spectrum recorded at the carbon core level (figure 4). It exhibits the bulk plasmon characteristic of the silicon carbide at 22.5 eV from the SiC C1s peak [11] (figure 4). The sp^2-carbon part remained unchanged compared to the 1073 K annealing. On the other hand, the remaining part of sp^3-carbon bonds is very weak, representing 3 % instead of 20 % previously. During this annealing, sp^3-carbon sites have been significantly modified. This will be further confirmed (Subsection 3.4).

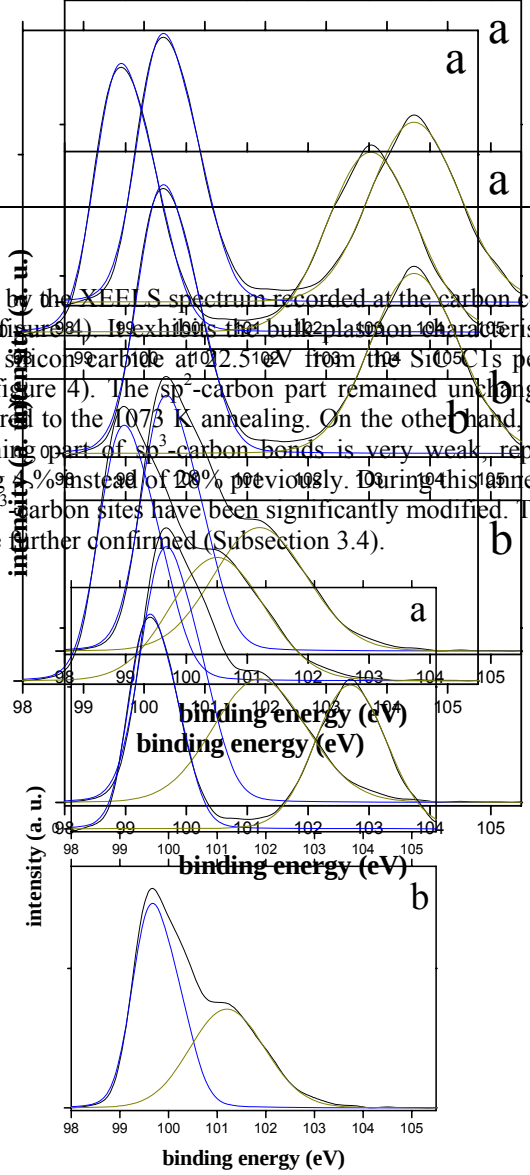

Figure 3 XPS Si 2p core level spectra after annealing a) at 1073 K; b) at 1173 K

Moreover, silicon oxide has been removed. This is well shown by the Si 2p core level (figure 3b). The previous oxide component has completely disappeared. The SiC component is now present at 101.1 eV. The thickness of the silicon carbide can be estimated from the ratio of XPS intensities assuming a continuous layer. The resulting value is lower than 1 nm which will be further discussed.

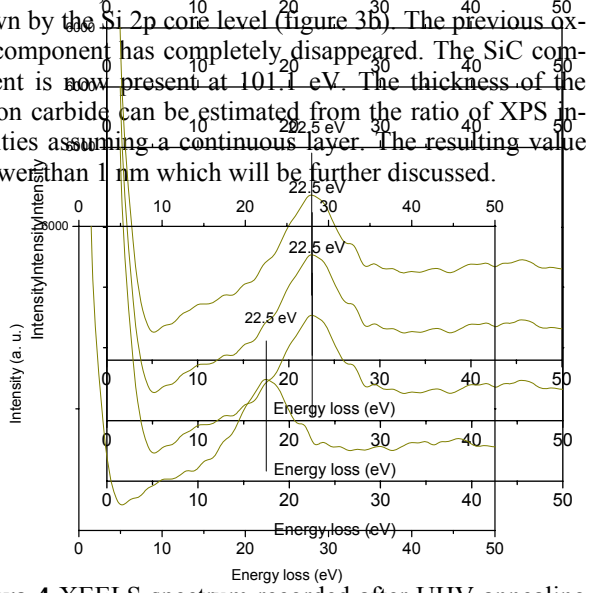

Figure 4 XEELS spectrum recorded after UHV annealing at 1173 K. The silicon carbide peak has been chosen as the energy loss origin.

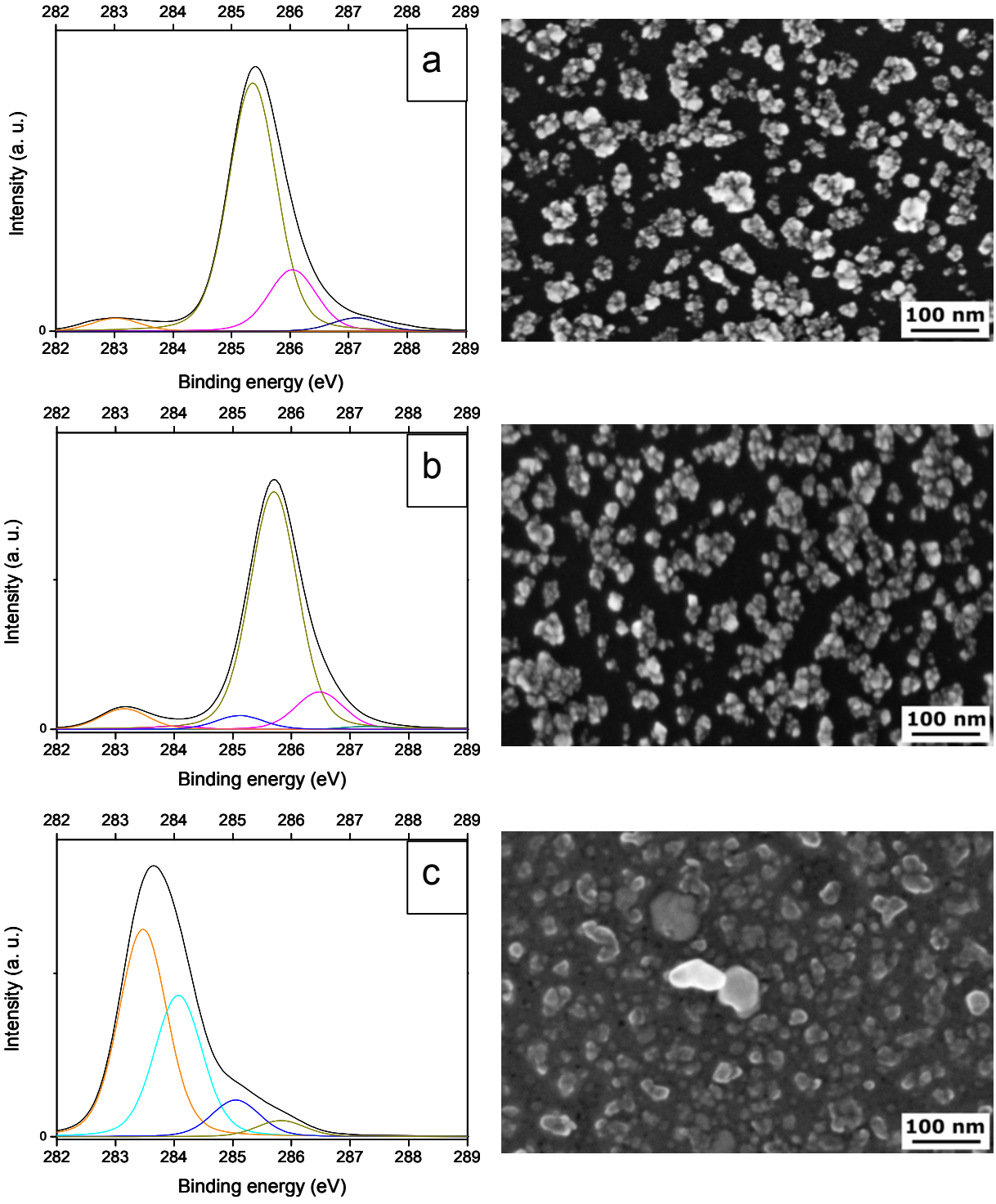

Figure 5 XPS C 1s core level spectra a) initial surface + 5 min growth b) 1073 K annealing + 5 min growth; c) 1173 K annealing + 5 min growth

3.4 Comparison of previous samples after a short growth step

The three previous samples underwent a short growth step. It has been applied to annealed samples to reveal the preserved sp^3 growth sites. The C 1s core level spectra and the corresponding FEG-SEM pictures are gathered on the figure 5.

The growth applied directly on the nanoseeded surface leads to a high density of diamond crystals. It has been estimated to 7.7 10^{10} / cm^2 from FEG-SEM pictures (figure 5a). The surface covered by diamond crystals is 26%. At the same time, the sp^3 component is the major one in the XPS C 1s spectrum.

Most of the sp^3-carbon sites have been preserved after the thermal annealing at 1073 K. Indeed, the FEG-SEM picture exhibits a density of crystals close to 8.9 10^{10} / cm^2 (figure 5b). It is quite comparable to the one obtained after the same growth step applied to nanoseeded silicon sample. The sp^3 component is the major one in the C1s core level spectrum, representing 75 % of the carbon amount probed by XPS (figure 5b).

On the other hand, for the sample annealed at 1173 K, the C 1s core level recorded after growth (figure 5c) did not exhibit so much modifications compared to the one recorded after UHV annealing (figure 1c). This confirms that the thermal treatment performed at 1173 K has strongly affected the sp^3 sites. Moreover, FEG-SEM investigations revealed a very different surface morphology. The features observed at the surface didn't show the same aspect than diamond crystals (figure 5). The XPS and XEELS spectra suggest these islands may correspond to silicon carbide crystals.

4 Discussion

According to surface analysis (XPS, XEELS) and FEG-SEM investigations, nanoseeded Si surfaces underwent important modifications after the UHV thermal treatments performed at 1173 K. Our results underlined that several mechanisms are involved simultaneously: the silicon oxide removal and the desorption of carbon / oxygen bonds which terminate UDD initially.

At the initial stage, most of the silicon surface, 83%, is uncovered by diamond nanoparticles (figure 2). The Si 2p core level reveals an oxidized silicon surface. After the UHV annealing at 1073 K during 60 min, the oxide is still present (figure 3a) while it is completely removed at 1173 K (figure 3b). Previous studies of the native oxide removal by UHV thermal annealing underlined the oxide transformation started between 973 K and 1073 K [12, 13]. This process involves the formation of volatile SiO. Indeed, the oxide loss process can be represented by the following equation: $SiO_2+Si \rightarrow 2SiO(g)\uparrow$. This mechanism occurs via the formation of voids at the surface which propagates as shown by STM investigations [13]. According to our results, the main part of the oxide remained after 60 min at 1073 K. However, it is removed when the thermal annealing at 1073 K is prolonged up to 15 h. This may indicate a very slow kinetic for the oxide removal at 1073 K.

Hydroxyl, ether, carbonyl and carboxyl groups are the signature of UDD termination according to the C 1s core level spectrum (figure 1a). They were also characterized by FTIR studies [7-8]. At 1073 K, the carbon / oxygen bonds underwent weak modifications (figure 1b) while they are strongly removed after the annealing at 1173 K (figure 1c). Their cumulate P_x/C_{total} ratio become negligible, close to 3%, compared to 41 % at the initial stage.

The silicon carbide formation is the consequence of the two previous mechanisms. Indeed, silicon and carbon atoms are no more bonded to oxygen according to XPS so that the carbon / silicon interdiffusion can take place. During UHV thermal treatments, UDD constitutes the unique source of carbon. Here, it is important to discuss about the thermal stability of the diamond nanoparticles. Particle-size measurements performed by dynamic light scattering method have shown 94% of the colloidal particles had an average particle size of 6.6 nm [3]. Moreover, TEM studies have underlined the size of the sp^3 core close to 4 nm surrounded by a sp^2 shell. The thermal stability of so small sp^3 islands is expected to be very different from the bulk diamond. Our experiments indicate that the temperature threshold for UDD is located between 1073 and 1173 K. This temperature is higher compared to C_{60} deposited on silicon surfaces [14]. In this case, C_{60} started to react with silicon for T = 993 K.

The proposed scheme for the silicon carbide formation should be a carbon / silicon interdiffusion occurring in the vicinity of UDD. Taking into account the surface covered by UDD estimated to 17 % (figure 2), this may support why the model of the continuous SiC layer is inadequate to estimate the SiC thickness from XPS data. Moreover, the presence of a C-terminated SiC component (with a significant P_x / C_{total} ratio close to 40 %) at the carbon core level (Fig 5c) is an indication that the transformation of UDD leads to non-stoichiometric SiC islands.

We previously studied the behaviour of UDD on silicon surfaces under hydrogen microwave CVD plasma [5]. Diamond nanoparticles exhibited a higher stability after H_2 plasma at 1213 K. Indeed, diamond has been detected either by XPS and FEG-SEM after a short growth step. This

result may be surprising because under H_2 plasma conditions diamond nanoparticles underwent an etching by atomic hydrogen. These results suggest that the passivation of UDD by hydrogen is relevant. The formation of C-H bonds at the surface of diamond nanoparticles plays a protective role for sp^3-carbon seeds.

5 Conclusion

We investigated the thermal stability of Ultra Dispersed Diamond under UHV using a sequential surface analysis. After the thermal treatment at 1173K, most of the sp^3 sites have been transformed. XPS and XEELS spectra underlined the formation of silicon carbide at the surface. At this temperature, silicon oxide is removed and desorption of UDD oxygen termination is observed. These two mechanisms are driving forces for the silicon carbide formation. To investigate the intrinsic thermal stability of UDD, other substrates should be considered to avoid the carbon / silicon interdiffusion like SiC or TiC layers.

Moreover, diamond nanoparticles on silicon surfaces are less stable under annealing at 1173 K than under H_2 plasma performed at a comparable temperature. This result may be supported by the protective role of atomic hydrogen which can passivate the surface of diamond nanoparticles.

Acknowledgements
KH is a Postdoctoral Fellow of the Research Foundation – Flanders (FWO).

References

[1] J-I. Chao, E. Perevedentseva,P-H. Chung, K-K. Liu, C.-Y. Cheng, C.-C. Chang, and C.-L. in Cheng, Biophysical Journal **93** (2007) 2199–2208.
[2] M. Daenen, O.A. Williams, J. D'Haen, K. Haenen and M. Nesladek, Phys. Stat. Sol. (a) **203** (2006) 3005.
[3] O.A. Williams, O. Douheret, M. Daenen, K. Haenen, E. Osawa, M. Takahashi, Chem. Phys. Lett, **445** (2007), 255.
[4] A. Krüger, M. Osawa, G. Jarre, Y. Liang, J. Stegk, L. Lu, phys. stat. sol. (a) **204** (2007) 2881.
[5] J.C. Arnault, S. Saada, M. Nesladek, O.A. Williams, K. Haenen, P. Bergonzo, E. Osawa, Diam. Relat. Mater. (2008) doi:10.1016/j.diamond.2008.01.008
[6] L.A. Bursill, A.L. Fullerton, L.N. Bourgeois, Internat. J. Modern Phys. B **15** (2001) 4087.
[7] A. Krüger, F. Kataoka, M. Ozawa, T. Fujino, Y. Suzuki, A.E. Aleksenskii, A. Ya. Vul', E. Osawa, Carbon **43** (2005) 1722.
[8] X. Xu, Z. Yu, Y. Zhu and B. Wang, J. Solid State Chem. **178** (2005) 688.
[9] T.M. Parrill and Y.W. Chung, Surf. Science **243** (1991) 96.
[10] V. M. Bermudez, Phys. Stat. Sol. B **202** (1997) 447.
[11] R.J. Meilunas, R.P.H. Chang, S. Liu, M.M. Kappes, Appl. Phys. Lett. **59** (1991) 3461.
[12] Y. Wei, R. M. Wallace, A. C. Seabaugh, Appl. Phys. Lett. **69** (1996) 1270.
[13] V. Palermo and D. Jones, Mat. Sci. Eng. B **88** (2002) 220.
[14] L. Moro, A. Paul, D. C. Lorents, R. Malhotra, R. S. Ruoff, P. Lazzeri, L. Vanzetti, A. Lui, S. Subramoney, J. Appl. Phys. **81** (1997) 6141.